Surface Review and Letters, Vol. 14, No. 5 (2007) 927–934

World Scientific
www.worldscientific.com

STRUCTURE, THERMAL STABILITY, AND CO ADSORPTION PROPERTIES OF PD NANOPARTICLES SUPPORTED ON AN ULTRA-THIN SiO_2 FILM

J.-L. LU*,†, J. WEISSENRIEDER†, S. KAYA†, H.-J. GAO*,
S. SHAIKHUTDINOV†,‡ and H.-J. FREUND†
*Beijing National Laboratory of Condensed Matter Physics, Institute of Physics,
Chinese Academy of Sciences, PO Box 603, Beijing 100080, China
†Fritz-Haber-Institut der Max-Planck-Gesellschaft,
Faradayweg 4-6, 14195 Berlin, Germany
‡shaikhutdinov@fhi-berlin.mpg.de

Received 3 April 2007

Nucleation, growth, and thermal stability of Pd particles vapor-deposited on an ultra-thin crystalline silica film grown on Mo(112) have been studied by scanning tunneling microscopy, X-ray photoelectron spectroscopy, infrared reflection absorption spectroscopy, and temperature-programmed desorption of CO. No preferential nucleation of Pd on the silica film is found at room temperature deposition: the hemispherical Pd nanoparticles are homogenously dispersed on the support at all coverages studied ($0.01-1$ ML (mono layer)). The Pd particles are resistant toward sintering up to 700 K as judged by STM; however, CO adsorption studies have revealed surface chemical modification at temperatures as low as 550 K. Strong morphological changes are observed above 800 K (ultimately resulting in elongated rectangular islands at $\sim$1000 K), which is accompanied by strong alterations of CO adsorption properties. The results are rationalized in terms of Pd and Mo substrate interdiffusion at elevated temperatures, while the silica film basically preserves its structure.

Keywords: Model catalysts; palladium; silica; CO adsorption; thin oxide films; thermal stability.

1. Introduction

During the last decade, metal particles deposited onto well-ordered oxide thin films grown on refractory metal single crystals have been used as suitable model systems for heterogeneous catalysts.[1–5] The crystalline oxide films with a thickness varying from a few angstroms to as much as 10 nm can be prepared, which solves the experimentally constraining problem of sample charging typically observed on the single crystal oxide samples and thus facilitates the use of a rich variety of powerful electron spectroscopic and microscopic surface science techniques.

Silica (SiO_2) is one of the most widely used supports in catalysis. In addition, the properties of thin silica layers are essential in modern semiconductor technologies and electronic devices. Preparation of well-ordered films of silica using Mo(112) as a substrate has been recently reported.[6–14] Scanning tunneling microscopy (STM), infrared reflection absorption spectroscopy (IRAS), and X-ray photoelectron spectroscopy (XPS) studies combined with the density functional theory calculations showed that the film consists of a two-dimensional network of

‡Corresponding author.

corner sharing [SiO_4] tetrahedra, with one oxygen of each tetrahedron binding to the protruding Mo atoms of the Mo(112) surface.[13,14]

Highly dispersed palladium is a well-known catalyst for many hydrogenation and oxidation reactions. The nucleation and growth of Pd particles on oxide surfaces have been addressed in numerous studies, including thin films of Al_2O_3,[15,16] MgO,[17–19] Cr_2O_3,[20] FeO,[21] Fe_3O_4,[22,23] and single crystal surfaces of MgO(100),[24] α-Al_2O_3(0001),[25] ZnO(0001),[26] and TiO_2(110).[27–29] In some cases, hemispherical[27] or even spherical particles[29] were observed, but well-faceted hexagonal or trigonal shapes were observed in others.[16,22,24,28] In all cases, the particles grew three-dimensionally, except for very low Pd coverages.[21,26,27] It has also been also shown that the morphology of the Pd particles is altered upon heating. Surface restructuring (faceting),[22,23,30–33] sintering,[30–32] and encapsulation[33,34] have been observed on different oxide supports. At elevated temperatures, Pd migration into the thin films may also occur.[21,30,31,35]

Although the atomic structure of the silica film on Mo(112) was not well understood by that time, the Pd particles supported on these films were shown by Giorgi *et al.*[36] and Ozensoy *et al.*[37] as a suitable Pd/SiO_2 model system. Thermal stability of these model catalysts was addressed by Min *et al.*[31] During the last years, the preparation of the silica film has been significantly improved, whereby atomically flat silica surfaces with a well-defined atomic structure can be obtained.[13,14] Recently, we have reported on CO-induced sintering observed for Pd deposits on the silica film at low temperatures.[32] In continuation of this work, here we provide a detailed information on the structure, thermal stability, and CO adsorption properties of the Pd particles deposited at room temperature using STM, XPS, IRAS, and temperature-programmed desorption (TPD).

2. Experimental

The experiments were performed in two ultra-high vacuum (UHV) chambers (base pressure below 2×10^{-10} mbar). One chamber was equipped with an STM (Omicron), XPS (Scienta SES200 analyzer), an IR-spectrometer (Bruker i66/vs), and standard facilities for sample preparation. TPD studies were carried out in another chamber equipped with a differentially pumped mass spectrometer (QMS, Fision) and AES/LEED (Omicron).

The ultra-thin silica films were grown as follows[13,14]: The clean Mo(112) surface was exposed to 5×10^{-8} mbar of oxygen at 900 K for 5 min, followed by ca. 1.2 monolayer (ML) of Si vapor deposition in the same oxygen pressure and temperature. The sample was then annealed in vacuum to 1250 K for 5 min. The quality of the films was checked by STM, which showed atomically flat surface without any silica particles. The IR-spectra were measured with *p*-polarized light at 84° grazing angle of incidence (resolution $\sim 2\,cm^{-1}$).

The ingredients used for the preparation of the silica film and Pd/silica samples in the TPD chamber are identical to those used in the STM/IRAS-chamber. CO was exposed to the surface at ~90 K using a directional gas doser. Then the sample was placed ~0.5 mm from the nozzle of the QMS shield in order to avoid desorption signals from the heating wires. The temperature and linear heating rate were precisely controlled by the feedback system (Schlichting Phys. Instrum.). The temperature was measured by a type C thermocouple spot-welded to the edge of the Mo(112) crystal.

Palladium (99.99%, Goodfellow) was vapor-deposited at 300 K using a commercial evaporator (Focus EFM 3) with a deposition rate of *ca.* 0.1 ML/min, which was calibrated with microbalance or STM. For each Pd/silica sample, a new silica film was prepared. The STM images presented in the paper were taken at room temperature at the typical sample voltage *ca.* 2 V and tunneling current 0.2–0.5 nA.

3. Results and Discussion

At all Pd coverages studied (0.01–1 ML), the particles were found homogeneously distributed on the silica surface, both on the terraces and step edges. At 0.01 ML, the lateral size of the particles varies between 0.7 and 1.5 nm with the height around 0.6 nm (see Fig. 1(a)). This indicates that the Pd particles grow three-dimensionally from the onset. When the coverage is increased to 0.1 ML, the particle density increases while the mean particle size remains basically the same (cf. Figs. 1(a) and 1(b)). At 1 ML coverage, the particle size increases up to 2–3 nm in

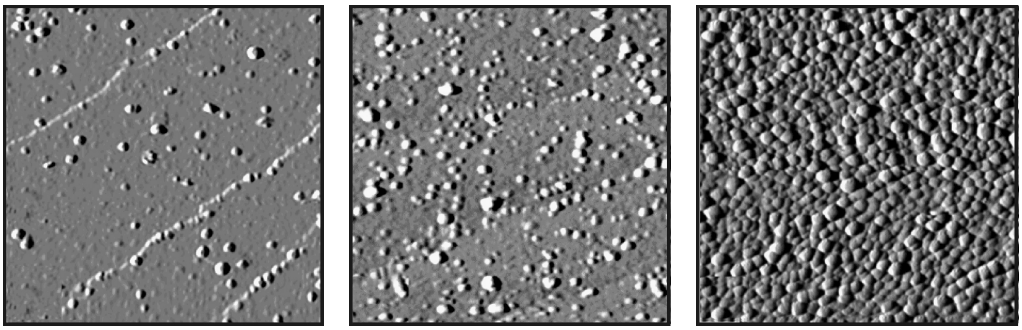

(a) (b) (c)

Fig. 1. STM images presented in differentiated contrast (size $80 \times 80\,\mathrm{nm}^2$) of 0.01 ML (a), 0.1 ML (b), and 1 ML (c) of Pd deposited on a silica film at 300 K.

diameter and ∼0.8 nm in height (see Fig. 1(c)). Bearing in mind the tip-sample convolution effect typically leading to overestimated lateral size, the aspect (height to diameter) ratio measured for the particles suggests that the Pd particles are hemispherical or rather ball-like in shape.

The surface structure of the Pd particles was probed by CO since the adsorption of CO on the Pd surfaces is well understood and a large database exists in the literature (Refs. 20, 23, 35–39 and references therein). Figure 2 shows CO IRAS spectra for the different Pd coverages at saturation CO exposure. The peak at $\sim 2095\,\mathrm{cm}^{-1}$, which dominates in the spectra at low coverage, can be assigned to CO adsorbing on the on-top sites of (111) facets and defect sites. The spectra basically scale at increasing Pd coverage up to 0.3 ML as shown in Fig. 2(b) where the spectra are normalized to the most intense peak at $\sim 2095\,\mathrm{cm}^{-1}$. This finding is consistent with the STM results showing that only the particle density increases in this range of coverage. The signal at $\sim 1938\,\mathrm{cm}^{-1}$ was previously assigned to CO on the bridge sites of Pd(111). At further increasing coverages, the band at $1962\,\mathrm{cm}^{-1}$ develops which corresponds to CO adsorbing at the bridge sites on Pd(100) facets, steps, and edge sites. The broad band, centered at $\sim 1840\,\mathrm{cm}^{-1}$, which is characteristic for CO adsorption in threefold hollow sites on Pd(111), appears only at high Pd coverage. The spectra at high Pd coverage are similar to those previously reported by Giorgi *et al.*[36] and also for Pd particles deposited on an alumina thin film at room temperature,[15,40] which mostly exposed the Pd(111) facets as resolved by STM.[16]

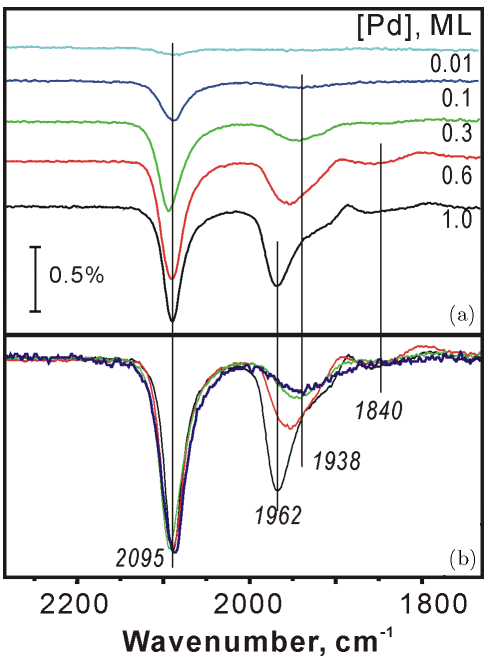

Fig. 2. (a) IRAS spectra of CO at saturated coverage as a function of Pd coverage as indicated (spectra are offset for clarity); (b) The same spectra normalized to the intensity of the peak at $2095\,\mathrm{cm}^{-1}$. 20 L of CO were dosed at 90 K for each spectrum.

A higher fraction of atop over multiply-coordinated CO species observed for Pd/SiO_2 than on Pd/Al_2O_3 at the same Pd coverage suggests that Pd nanoparticles exhibit less ordered surface structure, most likely due to the smaller size. Nonetheless, the IRAS results show that Pd particles deposited on the silica films become better-ordered at high Pd coverage.

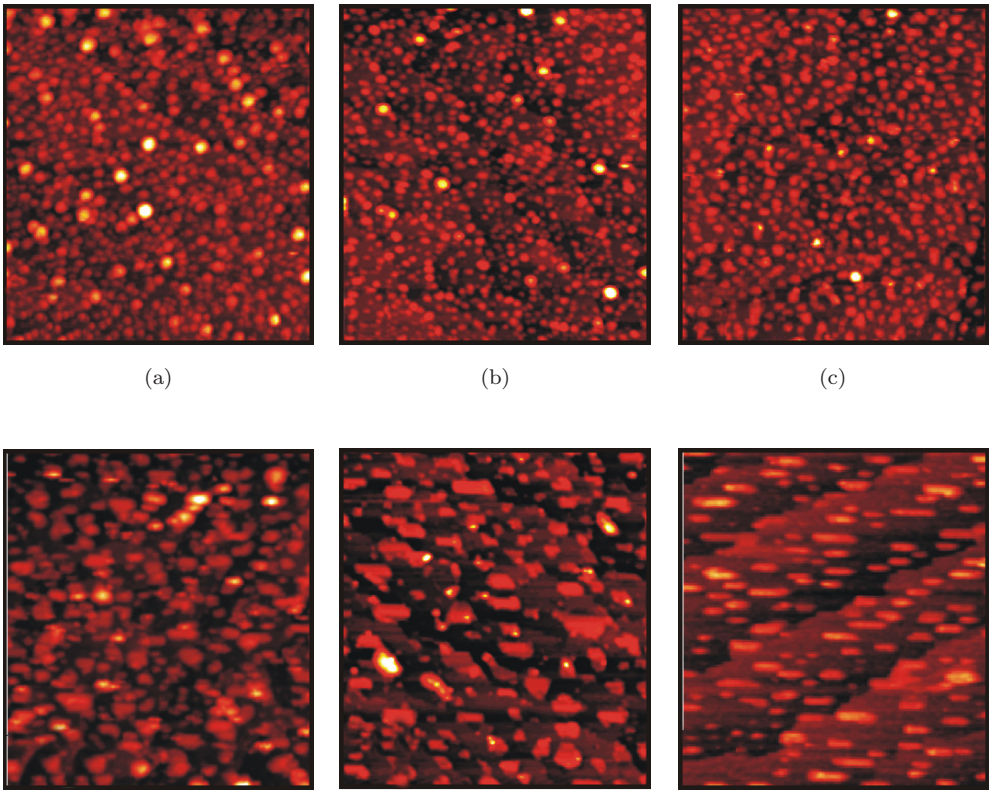

Fig. 3. Room temperature STM images ($100 \times 100\,\mathrm{nm}^2$) of the 0.3 ML Pd sample as deposited at 300 K (a) and after vacuum annealing to 600 (b), 800 (c), 900 (d), 970 (e), and 1050 K (f).

Figure 3 shows STM images of the 0.3 ML Pd sample taken after stepwise annealing in UHV. Up to 700 K, no significant changes in the particle size and density were observed. Pd undergoes strong sintering above 800 K, which results in significant decreasing of the particle density. In addition, the initially hemispherical particles sinter and become elongated in the direction that coincides with the [-1-11] direction of the Mo substrate. Figure 4 shows the high-resolution image of the rectangular islands observed in Fig. 3(f) which is *ca.* 12 nm in length but only 0.6 nm in height, i.e., two–three atomic layers of Pd. Interestingly, the elongated shape of metal particles on the silica films has been previously observed for Ag as-deposited at room temperature and assigned to a strong Ag–silica interaction.[41]

The annealed samples were further characterized by CO IRAS as shown in Fig. 5. Annealing to 450 K and further to 600 K results in simultaneous attenuation of all IR bands, which suggests reduction of the

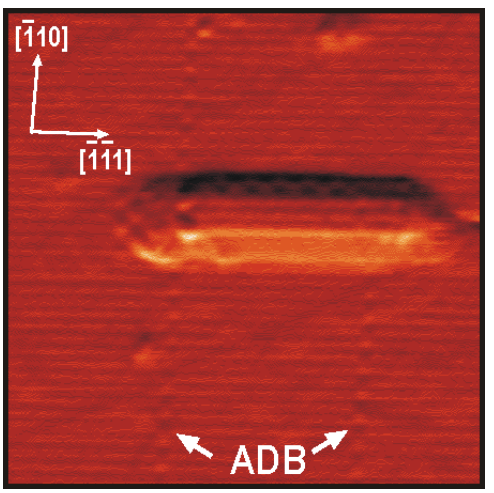

Fig. 4. High-resolution STM image ($18 \times 18\,\mathrm{nm}^2$) of the particle formed on the silica film upon annealing to 1050 K. The principle directions of the Mo(112) substrate are indicated. Antiphase domain boundaries (ADB) of the silica film are marked by arrows.

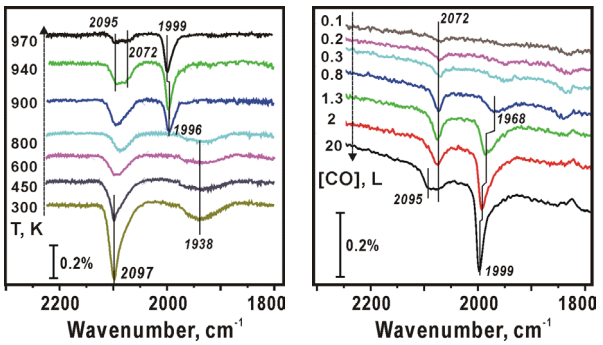

(a) (b)

Fig. 5. (a) CO IRAS spectra taken at 90 K for the 0.3 ML Pd sample prepared at 300 K and subsequently annealed in UHV to the indicated temperatures; (b) IRAS spectra for the sample annealed to 970 K as a function of CO exposure (in L) as indicated. The spectra are offset, for clarity.

Pd surface area either due to sintering of the particles or Pd disappearing from the surface. The STM results disfavor sintering of the particles at these temperatures. Note also, that the XPS study showed only ∼5% decrease in the integral intensity of the Pd-related photoelectron signals in the course of annealing indicating that Pd basically stays in the surface region.[32] Therefore, almost twofold reduction of the CO adsorption capacity as measured by IRAS upon heating to 600 K could, in principle, be attributed to an encapsulation of Pd by the silica which is essentially inert toward CO.

More dramatic changes occur upon heating above 800 K. The band at 1938 cm^{-1} vanishes and a new strong signal at 1996 cm^{-1} develops. In addition, the band centered at 2097 cm^{-1} deconvolutes into two bands, at 2095 cm^{-1} and at 2072 cm^{-1}. Figure 5(b) shows the IRA-spectra as a function of CO exposure for the sample annealed to 970 K. The high frequency band at 2072 cm^{-1} populates first, while the signal at 1968 cm^{-1} grows in intensity and shifts to the higher wave numbers. Finally, the signal at 2095 cm^{-1} emerges. Interestingly, the band at 1999 cm^{-1} and its CO coverage dependence are very similar to those observed for CO adsorption on Pd(100).[42] This, together with the observation of the rectangular particles at high temperatures, would seem to indicate the formation of Pd(100)-like islands on the silica. In order to check this hypothesis, we have performed TPD studies as CO desorption spectra on Pd(100) single crystal are well documented in the literature.[43,44]

TPD spectra at saturation CO exposure to the 1 ML Pd sample as a function of annealing temperature are shown in Fig. 6(a). For as-deposited Pd particles, the spectrum is similar to that previously observed for Pd on various oxide supports,[21,22,44,45] although the desorption signal at ∼465 K, assigned to the adsorption in threefold hollow sites on the Pd(111) facets,[46] is not so well pronounced as on other oxide films, which is consistent with the higher fraction of atop CO species. Annealing to 550 K significantly reduces the CO adsorption capacity mainly due to the loss of high temperature desorption states at $T > 400$ K. This effect gets stronger upon heating to 700 K. Simultaneously, a broad desorption peak

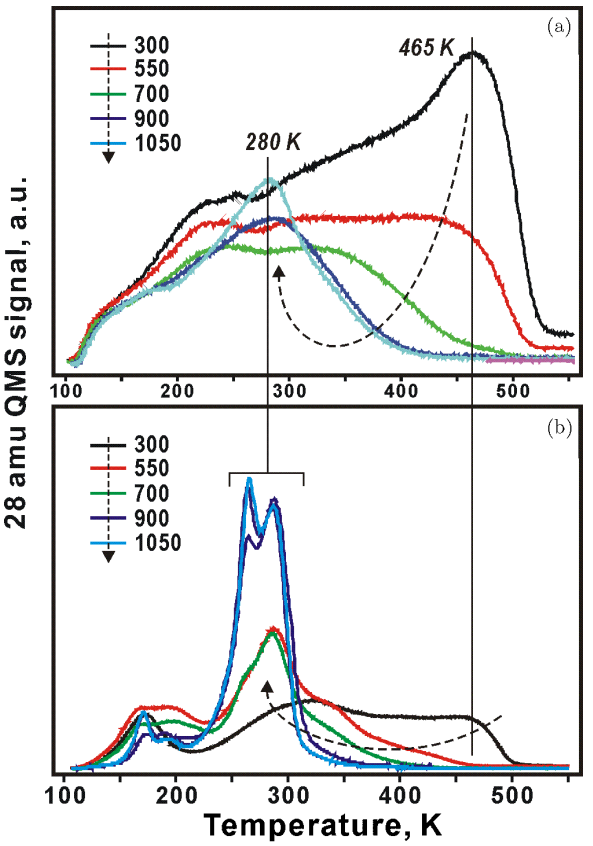

Fig. 6. CO TPD spectra of the 1 ML $Pd/SiO_2/Mo(112)$ and 1 ML Pd/Mo(112) surfaces after annealing to the indicated temperatures. A loss of the desorption states at $T > 400$ K simultaneously with the development of the signal centered at ∼280 K on heating is schematically shown by the arrows. 20 L of CO were dosed at ∼100 K in each spectrum.

centered at ~280 K develops, which grows in intensity at higher temperatures. Such TPD spectra have never been observed on pure Pd surfaces, therefore suggesting Pd intermixing with the substrate at and above 550 K.

Thermodynamic considerations preclude the reduction of silica by Pd and the formation of Pd-silicides. In agreement with Min *et al.*,[29] who observed the formation of Pd-silicides only after electron beam bombardment of the Pd/silica sample followed by annealing to 1000 K, we did not find any evidence for thermally induced Pd–Si alloying. Indeed, XPS measurements of the annealed samples showed no new features in the Si 2p region, which one would expect for Si ions in the $PdSi_x$ phase, i.e., very different from SiO_2. In addition, the Pd 3d region showed no significant changes in the peak position (within 0.1 eV) and only small (~5%) decrease in intensity.

On the other hand, the TPD spectra observed for the annealed Pd/silica samples are similar to those of a Pd monolayer supported on metal substrates (Refs. 47,48, and references therein). We have performed similar TPD experiments with 1 ML Pd deposited onto Mo(112) at 300 K, for comparison. As shown in Fig. 6(b), the thermally induced changes in the TPD spectra of Pd/Mo(112) show the same behavior as on Pd/SiO_2/Mo(112). Indeed, the desorption signal at ~465 K characteristic for CO on clean Pd surfaces disappears on heating. Meanwhile, the peak at around 285 K together with the shoulders at 260 and 340 K and broad signal at ~180 K are observed upon heating to 700 K. This latter spectrum is in fact very similar to the spectrum for Pd/silica annealed to 900 K (see Fig. 6(a)). The desorption states on Pd/Mo(112) become better resolved upon further heating above 900 K most likely due to better surface ordering.

The reduced CO binding energy on Pd monolayer formed on Mo(100) and Mo(110) substrates, previously observed by TPD and high resolution electron energy loss (HREELS) spectroscopy,[47,48] was described in terms of classical Blyholder model due to reduced back-donation between Pd 3d and the CO $2\pi^*$ orbital. In particular, the peak at 1950 cm^{-1} observed for 1 ML Pd/Mo(110), associated with the bridge sites, was disappearing at a lower temperature than the peak at 2085 cm^{-1} (i.e., atop species), indicating a higher binding energy for CO adsorbed on the on-top sites as compared to multicoordinated sites,[47] i.e., in agreement with theoretical predictions.[49]

Finally, Fig. 7 shows the vibrational spectra of the silica film in the phonon region (600–1100 cm^{-1}) which is sensitive to the structure of the films.[50] Pd deposition attenuates and shifts the main phonon signal at 1059 cm^{-1}, assigned to Si–O–Mo asymmetric stretching vibrations,[13,14] to the lower energies (1000 cm^{-1}). This effect is typically observed for metal overlayers on oxide films (see Refs. 51, and references therein) and assigned to a metallic screening (image dipole) mechanism. Subsequent annealing of the sample gradually shifts the main phonon almost back to the original frequency, increases the integral intensity, and reduces the bandwidth. Since wetting of the Pd overlayer is expected to result in even stronger attenuation of the substrate vibrational modes,[51] this finding is in principle consistent with the metal migration under the film, whereby the film preserves its structure.

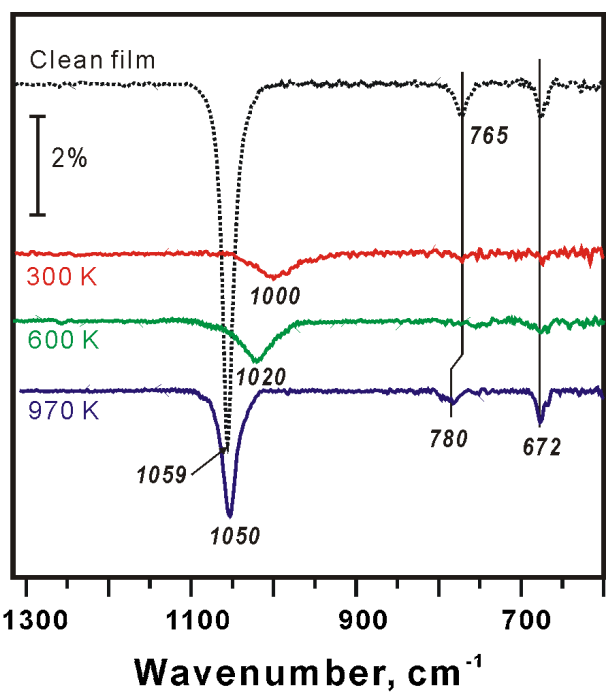

Fig. 7. Phonon region of the IRAS spectra taken at 90 K for the 0.3 ML Pd sample prepared at 300 K and subsequently annealed in UHV to the indicated temperatures. The spectrum for the clean silica film is shown, for comparison. The spectra are offset, for clarity.

Therefore, the results show that Pd particles deposited on the silica film undergo not only morphological but also strong chemical surface modifications at elevated temperatures. The combined results favor the conclusion that Pd intermixes with Mo substrate rather than with silica film. It seems plausible that Pd migrates to the silica/Mo interface as theoretically predicted for Pd single atoms.[52]The honeycomb-like structure of the silica film, which is only 1 ML in thickness, allows the metal ad-atoms to diffuse through the film without any barrier. However, it appears that Pd remains on the surface of the particles observed by STM since Pd has a lower surface energy than Mo, on an average.[53] Nonetheless, the presence of Mo in the "subsurface" region strongly affects the CO adsorption properties of Pd deposits. The Pd–Mo alloying which commences at ∼500 K may play a crucial role in the reactivity of these model catalysts, and in particular may partially explain the observation of CO dissociation reported by Ozensoy *et al.*[37] at elevated pressures.

Recently we have succeeded in the growth of the multilayer silica films, which showed very smooth topography (corrugation amplitude below 0.1 nm) and vibrational properties of bulk silica.[54] Pd particles deposited on these films showed typical sintering behavior on heating, and CO adsorption did not reveal any alloying of Pd with the support. These results suggest that thermal stability of the metal supported on the silica films is most probably governed by the thickness of the film.

4. Summary

Nucleation, growth, and thermal stability of Pd particles vapor-deposited onto ultra-thin silica film grown on Mo(112) have been studied by STM, XPS, IRAS, and TPD of CO. Pd particles grow three-dimensionally from the onset. The hemispherical Pd nanoparticles are homogenously distributed on the silica at all coverages studied (0.01–1 ML). The particles become better ordered and predominantly expose (111) facets at high coverage. The Pd particles are resistant toward sintering at $T <$ 700 K as judged by STM; however CO adsorption IRAS and TPD studies have revealed surface modification at ∼550 K. Much stronger morphological and CO adsorption changes are observed at higher temperatures, ultimately resulting in thin elongated islands at ∼1000 K. The combined results suggest that Pd particles undergo not only morphological but also strong chemical modifications, which have been assigned to Pd and Mo intermixing through the film whereby the silica film preserves its structure. Growth of the thicker silica films precludes strong interaction with the support and enhances thermal stability of the metal supported on the silica films.

Acknowledgments

The authors would like to acknowledge the support by the National Project 973 and the Natural Science Foundation of China (Grant 90406022) and the EU Project GSOMEN (NMP-CT-2004-001594). J.-L. L and S. K. thank the International Max-Planck Research School (IMPRS) "Complex Surfaces in Materials Science" and J. W. Alexander von Humboldt Foundation for fellowships.

References

1. D. W. Goodman, *Chem. Rev.* **95** (1995) 523.
2. C. T. Campbell, *Surf. Sci. Rep.* **27** (1997) 1.
3. R. Franchy, *Surf. Sci. Rep.* **38** (2000) 195.
4. C. Henry, *Surf. Sci. Rep.* **31** (1998) 231.
5. H.-J. Freund, *Surf. Sci.* **500** (2002) 271.
6. T. Schroeder, M. Adelt, B. Richter, M. Naschitzki, M. Baümer and H.-J. Freund, *Surf. Rev. Lett.* **7** (2000) 7.
7. T. Schroeder, J. B. Giorgi, M. Bäumer and H.-J. Freund, *Phys. Rev. B* **66** (2002) 165422.
8. B. K. Min, A. K. Santra and D. W. Goodman, *Catal. Today* **85** (2003) 113.
9. M. S. Chen, A. K. Santra and D. W. Goodman, *Phys. Rev. B* **69** (2004) 155404.
10. B. K. Min, W. T. Wallace, A. K. Santra and D. W. Goodman, *J. Phys. Chem. B* **108** (2004) 16339.
11. B. K. Min, W. T. Wallace and D. W. Goodman, *J. Phys. Chem. B* **108** (2004) 14609.
12. S. Wendt, E. Ozensoy, T. Wei, M. Frerichs, Y. Cai, M. S. Chen and D. W. Goodman, *Phys. Rev. B* **72** (2005) 115409.
13. J. Weissenrieder, S. Kaya, J.-L. Lu, H.-J. Gao, S. Shaikhutdinov, H.-J. Freund, M. Sierka, T. K. Todorova and J. Sauer, *Phys. Rev. Lett.* **95** (2005) 076103.
14. T. K. Todorova, M. Sierka, J. Sauer, S. Kaya, J. Weissenrieder, J.-L. Lu, H.-J. Gao, S. Shaikhutdinov and H.-J. Freund, *Phys. Rev. B* **73** (2006) 165414.
15. M. Frank and M. Bäumer, *Phys. Chem. Chem. Phys.* **2** (2000) 3723.
16. K. H. Hansen, T. Worren, S. Stempel, E. Lægsgaard, M. Bäumer, H.-J. Freund, F. Besenbacher and I. Stensgaard, *Phys. Rev. Lett.* **83** (1999) 4120.

17. G. Haas, A. Menck, H. Brune, J. V. Barth, J. A. Venables and K. Kern, *Phys. Rev. B* **61** (2000) 11105.
18. J. A. Venables, L. Giordano and J. H. Harding, *J. Phys.: Condens. Matter* **18** (2006) 411.
19. C. Xu, W. S. Oh, G. Liu, D. Y. Kim and D. W. Goodman, *J. Vac. Sci. Technol. A* **15** (1997) 1261.
20. K. Wolter, H. Kuhlenbeck and H.-J. Freund, *J. Phys. Chem. B* **106** (2002) 6723.
21. R. Meyer, M. Bäumer, S. Shaikhutdinov and H.-J. Freund, *Surf. Sci.* **546** (2003) L813.
22. R. Meyer, S. Shaikhutdinov and H.-J. Freund, *Z. Phys. Chem.* **218** (2004) 905.
23. T. Schalow, B. Brandt, S. E. Starr, M. Laurin, S. Schauermann, S. K. Shaikhutdinov, J. Libuda and H.-J. Freund, *Catal. Lett.* **107** (2006) 189.
24. C. R. Henry, C. Chapon, C. Duriez and S. Giorgio, *Surf. Sci.* **253** (1991) 177.
25. C. L. Pang, H. Raza, S. A. Haycock and G. Thornton, *Surf. Sci. Lett.* **460** (2000) L510.
26. H. Jacobs, W. Mokwa, D. Kohl and G. Heiland, *Surf. Sci.* **160** (1985) 217.
27. C. Xu, X. Lai, G. W. Zajac and D. W. Goodman, *Phys. Rev. B* **56** (1997) 13464.
28. P. Stone, R. A. Bennett, S. Poulston and M. Bowker, *Surf. Sci.* **433** (1999) 501.
29. M. J. J. Jak, C. Konstapel, A. Van Kreuningen, J. Verhoeven and J. W. M. Frenken, *Surf. Sci.* **457** (2000) 295.
30. M. Heemeier, S. Stempel, S. Shaikhutdinov, J. Libuda, M. Bäumer, R. J. Oldman, S. D. Jackson and H.-J. Freund, *Surf. Sci.* **523** (2003) 103.
31. B. K. Min, A. K. Santra and D. W. Goodman, *J. Vac. Sci. Technol. B* **21** (2003) 2319.
32. J.-L. Lu, S. Kaya, J. Weissenrieder, H.-J. Gao, S. Shaikhutdinov and H.-J. Freund, *Surf. Sci. Lett.* **600** (2006) L153.
33. O. Dulub, W. Hebenstreit and U. Diebold, *Phys. Rev. Lett.* **84** (2000) 3646.
34. M. Bowker, P. Stone, R. Bennett and N. Perkins, *Surf. Sci.* **497** (2002) 155.
35. A. Sandel, J. Libuda, M. Bäumer and H.-J. Freund, *Surf. Sci.* **346** (1996) 108.
36. J. B. Giorgi, T. Schroeder, M. Bäumer and H.-J. Freund, *Surf. Sci. Lett.* **498** (2002) L71.
37. E. Ozensoy, B. K. Min, A. K. Santra and D. W. Goodman, *J. Phys. Chem. B* **108** (2004) 4351.
38. F. M. Hoffman, *Surf. Sci. Rep.* **3** (1983) 107.
39. I. V. Yudanov, R. Sahnoun, K. M. Neyman *et al.*, *J. Phys. Chem. B* **107** (2003) 255.
40. K. Wolter, O. Seiferth, H. Kuhlenbeck, M. Bäumer and H. -J. Freund, *Surf. Sci.* **399** (1998) 190.
41. A. K. Santra, B. K. Min and D. W. Goodman, *Surf. Sci.* **515** (2002) L475.
42. A. Ortega, F. M. Hoffman and A. M. Bradshaw, *Surf. Sci.* **119** (1982) 79.
43. E. M. Stuve, R. J. Madix and C. R. Brundle, *Surf. Sci.* **146** (1984) 155.
44. R. J. Behm, K. Christmann, G. Ertl and M. A. van Hove, *J. Chem. Phys.* **73** (1980) 2984.
45. S. Shaikhutdinov, M. Heemeier, J. Hoffmann *et al.*, *Surf. Sci.* **501** (2002) 270.
46. X. Guo and J. T. Yates Jr., *J. Chem. Phys.* **90** (1989) 6761.
47. C. Xu and D. W. Goodman, *Surf. Sci.* **360** (1996) 249.
48. J. M. Heitzinger, S. C. Gebhard and B. E. Koel, *Surf. Sci.* **275** (1992) 209.
49. S. Pick, *Chem. Phys. Lett.* **239** (1995) 84.
50. M. Sierka, T. K. Todorova, S. Kaya *et al.*, *Chem. Phys. Lett.* **424** (2006) 115.
51. M. Frank, K. Wolter, N. Magg, M. Heemeier *et al.*, *Surf. Sci.* **492** (2001) 270.
52. L. Giordano, A. D. Vitto and G. Pacchioni, *J. Chem. Phys.* **124** (2006) 034701.
53. L. Vitos, A. V. Ruban, H. L. Skriver and J. Kollar, *Surf. Sci.* **411** (1998) 186.
54. D. Stacchiola, M. Baron, S. Shaikhutdinov and H.-J. Freund, submitted to *Appl. Phys. Lett.*